

Numerical Study on the Shear Behaviour of Railway Ballast Using Discrete Element Method



S. Venuja, S. K. Navaratnarajah, W. R. R. Jayawardhana,
P. H. L. Wijewardhana, K. Nirmali, and M. A. M. Sandakelum

Abstract Rail transport is the most popular mode of transport where a large number of passengers and a large amount of freights are transported efficiently with economical benefits. Ballasted tracks are the widely used track foundation system around the world. Railway ballast is a coarse granular material with high bearing capacity and shear strength. The ballast layer uniformly transmits the loads from moving trains and sleepers to the underlying layers at a reduced level. When studying the behaviour of ballast under different loading conditions, a huge amount of ballast materials are consumed and it is very labour intensive work for large-scale laboratory tests. Nowadays, numerical studies are adopted by many researchers to reduce the usage of human resources and materials. And also, numerical studies enable extended analysis through conducting a parametric study using the validated model. In this study, a numerical model was developed to study the shear behaviour of ballast and ballast–concrete interface using the discrete element method. Ballast with different shapes and sizes were modelled using multi-sphere clumps. The model was run under 30, 60, and 90 kPa normal stresses with a constant shearing rate of 4 mm/min as same as the laboratory test conditions. The model was validated using previous experimental results, and an acceptable agreement was observed for the ballast–concrete interface. The formation of the shear band in direct shear loading was observed by analysing the contact force distribution and the displacement vectors. The validated model can be used to study the change in shear behaviour of ballast when geogrid is inserted. Further, the model can be improved to incorporate the breakage of ballast particles.

Keywords Discrete element method · Multi-sphere clumps · Railway ballast · Shear band · Shear behaviour

S. Venuja (✉) · S. K. Navaratnarajah · W. R. R. Jayawardhana · P. H. L. Wijewardhana · K. Nirmali · M. A. M. Sandakelum
Department of Civil Engineering, Faculty of Engineering, University of Peradeniya, Peradeniya, Sri Lanka
e-mail: venuvas@eng.pdn.ac.lk

1 Introduction

Rail transport is one of the most popular modes of land transport all over the world. Ballasted tracks and slab tracks are the two types of track systems on which trains are travelling. Even though the maintenance cost and frequency are higher for ballasted rail tracks than that for slab tracks, the former is highly adopted due to ease of construction, low initial investment, and good noise and vibration absorption [1, 2]. The enormous growth in population and urbanization increases the necessity for heavier and faster trains. Cyclic and impact loads generated by fast-moving heavy haul trains cause breakage, high lateral spread, and settlement of ballast, leading to rail–sleeper misalignment and loss of load-bearing capacity, and hence, compromised safety and frequent track maintenance [6, 8, 13, 15, 16, 19, 23].

Ballast material is placed underneath and around the sleepers and followed by sub-ballast and subgrade layers. The ballast layer is the largest layer by volume and weight in the track foundation system. The primary function of the ballast layer is to transfer the train-exerted loads to the underlying layers more uniformly at a minimal level and provide lateral safety to the rail tracks [14, 25, 27]. The high shear resistance of ballast is due to the rough surface texture and sharp edges of particles which give higher frictional resistance. When loads on the ballast layer increase, ballast undergoes breakage and smoothening of surface and edges, thus leading to a reduction in frictional resistance. Loss of shear resistance of the ballast layer leads to high lateral spreading and loss of track geometry. Ballast breakage depends on the interface types such as concrete–ballast, timber–ballast, ballast–ballast, ballast–rubber, ballast–geogrid, and so on [17, 18]. Therefore, it is necessary to analyse the shear behaviour of ballast with different interfaces. In this study, a numerical model was developed to analyse the shear behaviour of ballast and validated using the results from a previous experiment-based study [17] carried out on a large-scale direct shear apparatus.

2 Numerical Modelling

2.1 Literature Review

Adaptation of numerical modelling is developed over years with the advancements in computational power within a short period of time. The common types of numerical approaches are the Finite Element Method (FEM) and the Discrete Element Method (DEM). FEM is a continuum numerical method that has domains with boundary conditions whereas DEM is a discrete approach that analyses the macroscopic behaviour of the system from individual particle interactions.

Modelling of ballast in FEM purely depends on the material model adopted to mimic the nature of ballast material. Chawla et al. [3], Fattah et al. [7], Indramohan et al. [10], Jiang and Nimbalkar [12], Navaratnarajah et al. [20], Ramos et al. [22],

and Varandas et al. [26] are a few of the numerical studies carried out on ballast using FEM. Indramohan et al. [10] developed a model using FEM to calibrate the triaxial testing on railway ballast. 150 mm diameter and 600 mm high cylindrical model was used to represent the ballast. Since ballast shows elastoplastic failure, elastic and Drucker–Prager yielding properties were assigned as ballast material properties. This developed model produced similar results with the experimental results up to 120 kPa confining pressure and this study suggested that the FEM is useful in analysing the behaviour of ballast and other track components under different loading conditions.

Many other numerical studies have been carried out on ballast under various loading conditions using DEM [4, 5, 9, 11, 21, 24, 28]. Ngo et al. [21] developed a numerical model in DEM to simulate the fouled ballast behaviour with geogrid insertion under shear loading. Ballast aggregates with different shapes were created by connecting several spheres of various sizes and positions, and a library with different particle shapes was generated. Biaxial and triaxial geogrids were created by bonding small spheres (4 mm diameter balls at ribs and 8 mm diameter balls at junctions) using contact and parallel bonds. Coal fouling was adopted by inserting several 1.5 mm spheres into the voids of fresh ballast considering the contamination percentage. Normal stress was applied using a top-loading plate under a numerical servo-control mechanism. DEM models of fresh and coal-fouled ballast were in good agreement with the experimental results and minor deviations resulted from the rigidity of the top-loading plate and inadequate capturing of particle breakage. Coal fines reduced the interlocking of ballast particles into the geogrid apertures; thus, a reduction in the shear strength was observed.

2.2 Significance of Modelling Ballast by DEM

The limitations of FEM in modelling ballast are no exact material model that can exactly reflect the elastoplastic and discrete properties of ballast, difficulty to obtain the displacements and deformations, and not considering ballast breakage. DEM is capable to capture the microscopical and macroscopical behaviour of granular materials. It captures the complete particle information during the numerical simulations, considers the characteristics of individual ballast particles, and understands the effects of ballast particle degradation on the performance and deformation of the entire system. But DEM consumes more computational time when considering complex particle shapes, particle breakage, and a large number of loading cycles together. Therefore, there are only limited studies on railway ballast performance analysis using DEM.

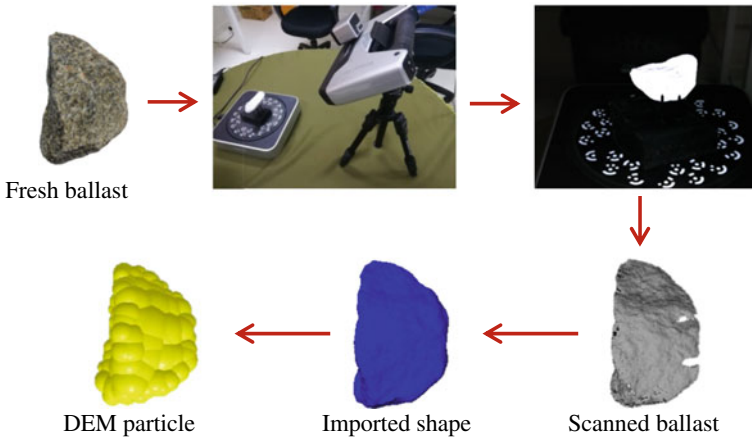


Fig. 1 Particle generation procedure in DEM with actual shapes

2.3 Particles Generation

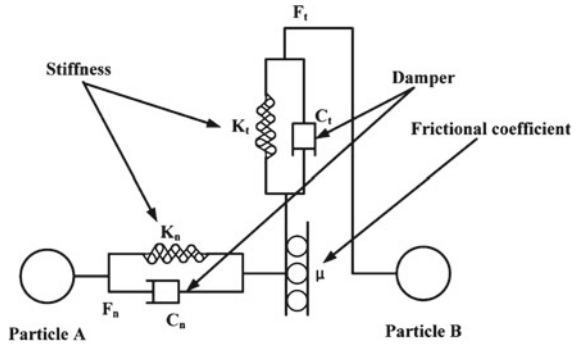
Computational time primarily depends on the complexity of the particle shape; therefore, particle shape should be simple enough as well as efficiently represent the real shape. When the real shape of a particle is used in numerical simulation, that model can produce more realistic outcomes. Therefore, the 3D scanning method was used to adopt the actual shape of the ballast particle in the numerical model. Three representative ballast aggregates each from four different particle size intervals within the gradation of ballast selected. Initially, the selected ballast aggregates were washed, air-dried, and painted with mat type of white colour paint. A 3D laser scanner (EinScan-Pro) was used to capture the irregular shape of the ballast aggregate in the form of point cloud data. Then, a closed surface was established and sphere balls were randomly generated using the radius expansion method inside it to make DEM particles as elaborated in Fig. 1.

A solid density of 2680 kg/m^3 and Poisson's ratio of 0.35 were used for ballast material. Particle size distribution was defined as the same as used in the laboratory tests. A constant mass loading rate was applied to a virtual injector to fill the apparatus with a predetermined mass of ballast particles.

2.4 Contact Modelling

Particle to particle and particle to geometry are the two interactions considered in DEM. The accuracy of DEM results is highly influenced by the contact model parameters. Unbreakable particles were created using the multi-sphere method where an infinity bond is between spheres inside a particle. DEM commonly uses simplified

Fig. 2 Hertz-Mindlin contact model



contact models that find the forces acting on a particle due to contact within an efficient computational time. A linear contact model was used to simulate the interaction between ballast particles and particles to geometry. Figure 2 illustrates the Hertz-Mindlin contact model which is used to provide an accurate and deep understanding of granular motion contacts of ballast particles.

2.5 Test Apparatus Modelling

A large-scale direct shear apparatus was modelled numerically in this study. The dimensions and components of the apparatus can be found elsewhere [17]. The main three components are the lower part, upper part, and top-loading plate and are shown in Fig. 3. The thickness of the top and bottom parts of the shear box is kept as 60 mm to keep the ballast sample inside the apparatus while the shear boxes are moving, but it does not affect the real testing procedure. Steel is used as the equipment material of these three parts. The upper part is stationary and the lower part is movable in the shearing direction with a constant velocity of 4 mm/min. Both upper and lower parts are vertically immovable. The top-loading plate is used to apply normal stresses on ballast during the test.

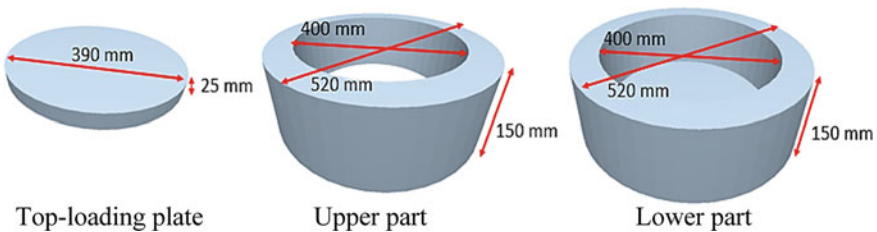


Fig. 3 Major components in the numerical model of the large-scale direct shear apparatus

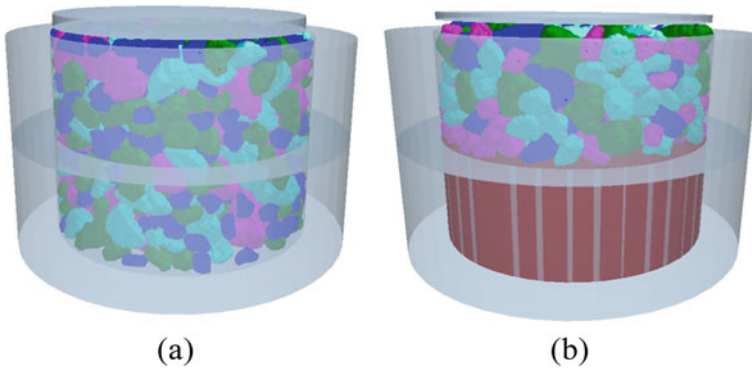


Fig. 4 **a** Model of ballast–ballast interface test; **b** Model of ballast–concrete interface test

Figure 4a shows the particle-filled model used to analyse the ballast shear behaviour. For the concrete–ballast interface test, a concrete cylinder was placed completely in the lower part of the cylinder as shown in Fig. 4b. Thus, in the numerical model also a solid cylinder geometry with concrete properties was used at the lower part. On top of it, ballast particles were filled.

3 Model Validation

A three-dimensional discrete element model is used to predict the shear behaviour of the ballast–ballast interface and ballast–concrete interface. Based on the results, the ballast–ballast interface exhibited higher shear resistance than that of the ballast–concrete interface (see Fig. 5). This was due to the higher interlocking nature of ballast aggregates which produced higher resistance to shear loading.

In numerical results, shear stress increased with the normal stress increment regardless of the type of interface (see Figs. 6 and 7). This is due to the increase in particle rolling and interlocking which results in higher resistance to shear loading. When comparing the numerical results with the experimental results, the ballast–concrete interface gave an acceptable agreement compared with the ballast–ballast interface. In this numerical method, ballast particle breakage was not taken into account and the material properties were used exactly the same as the ballast properties obtained from laboratory tests. These may considerably affect the numerical results in the ballast–ballast interface as shown in Fig. 6. In ballast–concrete interface shear behaviour, after attaining higher shear stress between 0 and 4% of shear strain, a minimal increase in shear stress was observed between 4 and 15% of shear strain in experimental results under all three normal stresses. A similar trend was observed in numerical results as shown in Fig. 7.

Fig. 5 Shear stress variation of ballast–ballast and ballast–concrete interfaces [17]

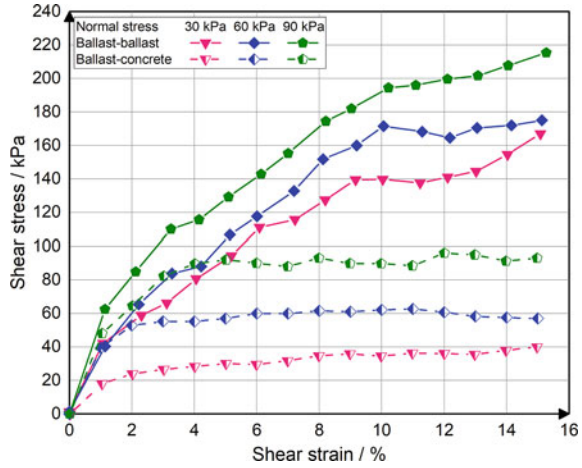
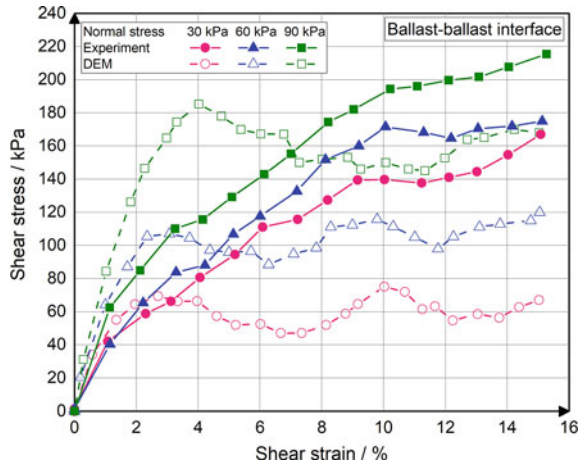


Fig. 6 Comparison of numerical and experimental results of ballast–ballast interface



4 Conclusions

Ballast particles with different shapes were created using the multi-sphere method by bonding several spheres with various diameters together. The shear behaviour of ballast–ballast and ballast–concrete interfaces under three different normal stresses was observed. Shear stress increased with higher normal stresses for both interfaces. Higher shear stress was obtained for the ballast–ballast interface than that of the ballast–concrete interface under the same normal stress. This higher shear resistance results from the increased particle interlocking at the ballast–ballast interface. The numerical model produced results that were acceptably matched with the experimental results. For more agreement with the experimental results, it is essential to use some different properties of ballast for spheres to get the real ballast

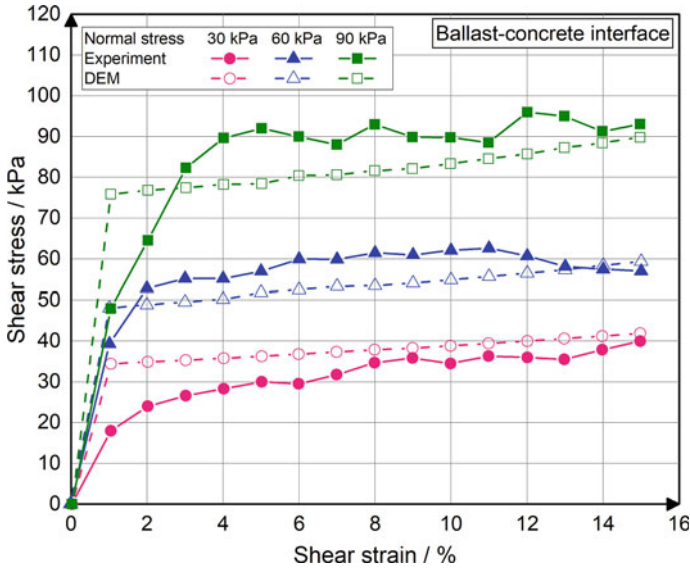


Fig. 7 Comparison of numerical and experimental results of ballast–concrete interface

behaviour in discrete element modelling when using the multi-sphere method to develop ballast particles. And also, ballast particles created in this simulation are unbreakable. Therefore, this model could not exhibit the breakage behaviour of ballast.

Acknowledgements The financial support provided by the Accelerating Higher Education Expansion and Development (AHEAD) Operation of the Ministry of Higher Education funded by the World Bank (Grant No: AHEAD/RA3/DOR/STEM/No.63) is appreciated. The support from the University of Peradeniya Research Grant (Grant No.: URG-2017-29-E) is also acknowledged.

References

- Al-Douri YK, Tretten P, Karim R (2016) Improvement of railway performance: a study of Swedish railway infrastructure. *J Mod Transp* 24(1):22–37
- Alemu AY (2011) Survey of railway ballast selection and aspects of modelling techniques. Master degree. Royal Institute of Technology. Available at:
- Chawla S, Banerjee L, Dash SK (2018) Three dimensional finite element analyses of geocell reinforced railway tracks. In: Indian geotechnical conference. Bengaluru, India, pp 1–5
- Chen C, McDowell GR, Thom N (2013) A study of geogrid-reinforced ballast using laboratory pull-out tests and discrete element modelling. *Geomech Geoeng* 8(4):244–253
- Dahal B, Mahmud SN, Mishra D (2018) Simulating ballast breakage under repeated loading using the discrete element method. In: ASME/IEEE joint rail conference. American Society of Mechanical Engineers, p V001T01A003
- Ebrahimi A, Tinjum JM, Edil TB (2015) Deformational behavior of fouled railway ballast. *Can Geotech J*. [https://doi.org/10.1139/cgj-2013-027152\(3\),344-355](https://doi.org/10.1139/cgj-2013-027152(3),344-355)

7. Fattah MY, Mahmood MR, Aswad MF (2017) Experimental and numerical behavior of railway track over geogrid reinforced ballast underlain by soft clay. In: International Congress and exhibition - sustainable civil infrastructures: innovative infrastructure geotechnology. Springer, Berlin, pp 1–26
8. Guo Y, Zhao C, Markine V, Jing G, Zhai W (2020) Calibration for discrete element modelling of railway ballast: a review. *Transp Geotech.* <https://doi.org/10.1016/j.trgeo.2020.100341>
9. Hossain Z, Indraratna B, Darve F, Thakur P (2007) DEM analysis of angular ballast breakage under cyclic loading. *Geomech Geoeng: Int J* 2(3):175–181
10. Indramohan SA, Goswami P (2016) Stress strain behavior of railway ballast under static loading using finite element method. *Int J Sci Eng Res* 7(12):7–10
11. Indraratna B, Thakur PK, Vinod JS (2010) Experimental and numerical study of railway ballast behavior under cyclic loading. *Int J Geomech* 10(4):136–144
12. Jiang Y, Nimbalkar SS (2019) Finite element modelling of ballasted rail track capturing effects of geosynthetic inclusions. *Front Built Environ* 5:69 (01–11)
13. Juhasz E, Fischer S (2019). Specific evaluation methodology of railway ballast particles' degradation. Science and transport progress. *Bull Dnipropetrovsk Natl Univ Railway Transp* 0(3(81)):96–109. <https://doi.org/10.15802/stp2019/171778>
14. Le Pen LM, Powrie W (2011) Contribution of base, crib, and shoulder ballast to the lateral sliding resistance of railway track: a geotechnical perspective. *Proc Inst Mech Eng, Part F: J Rail Rapid Transit.* [https://doi.org/10.1177/0954409710397094225\(2\),113-128](https://doi.org/10.1177/0954409710397094225(2),113-128)
15. Mishra A, Goyal S, Muttharam M, Nanthakumar S (2018) Study on the performance of railway ballasted track reinforced with geogrid. *Indian J Sci Technol.* 11(23):1–4. <https://doi.org/10.17485/ijst/2018/v11i23/114374>
16. Navaratnarajah S, Indraratna B, Nimbalkar S (2015) Performance of rail ballast stabilized with resilient rubber pads under cyclic and impact loading. In: International conference on geotechnical engineering. Colombo, pp 617–620
17. Navaratnarajah SK, Gunawardhana KRCM, Gunawardhana MASP (2019) Influence of type of interfaces on railway ballast behavior. In: ICSECM 2019, lecture notes in civil engineering. Springer, Berlin, pp 243–251
18. Navaratnarajah SK, Indraratna B (2020) Application of under sleeper pads to enhance the sleeper-ballast interface behaviours. In: Construction in geotechnical engineering. Springer, Singapore, pp 619–636
19. Navaratnarajah SK, Indraratna B (2020) Stabilisation of stiffer rail track substructure using artificial inclusion. *Indian Geotech J* 50(2):196–203
20. Navaratnarajah SK, Indraratna B, Ngo NT (2018) Influence of under sleeper pads on ballast behavior under cyclic loading: experimental and numerical studies. *J Geotech Geoenviron Eng* 144(9):1–16
21. Ngo NT, Indraratna B, Rujikiatkamjorn C (2014) DEM simulation of the behaviour of geogrid stabilised ballast fouled with coal. *Comput Geotech.* <https://doi.org/10.1016/j.compgeo.2013.09.00855,224-231>
22. Ramos A, Correia AG, Calçada R, Costa PA, Esen A, Woodward P, Connolly D, Laghrouche O (2021) Influence of track foundation on the performance of ballast and concrete slab tracks under cyclic loading: Physical modelling and numerical model calibration. *Constr Build Mater* 277:122245
23. Shih JY, Thompson DJ, Zervos A (2017) The influence of soil nonlinear properties on the track/ground vibration induced by trains running on soft ground. *Transp Geotech.* <https://doi.org/10.1016/j.trgeo.2017.03.00111,1-16>
24. Sluganović V, Lakušić S, Lazarević D (2019) Track ballast modelling by discrete element method. *Gradevinar* 7:589–600. <https://doi.org/10.14256/JCE.2350.2018>
25. Sweta K, Hussaini SKK (2018) Effect of shearing rate on the behavior of geogrid-reinforced railroad ballast under direct shear conditions. *Geotext Geomembr* 46(3):251–256
26. Varandas J, Paixão A, Fortunato E, Coelho BZ, Hölscher P (2020) Long-term deformation of railway tracks considering train-track interaction and non-linear resilient behaviour of aggregates—a 3D FEM implementation. *Comput Geotech* 126:103712

27. Venuja S, Navaratnarajah SK, Bandara CS, Jayasinghe JASC (2019) Review on geosynthetic inclusions for the enhancement of ballasted rail tracks. In: ICSECM 2019, Lecture notes in civil engineering. Springer, Berlin, pp 459–468
28. Zhao H, Chen J (2020) A numerical study of railway ballast subjected to direct shearing using the discrete element method. *Adv Mater Sci Eng.* <https://doi.org/10.1155/2020/340420820> 20,1-13